NRC Research Press

ARTICLE

A combined kinetic and computational study of the reactions of transient germylenes with oxiranes and thiiranes in solution

Svetlana S. Kostina and William J. Leigh

Abstract: The reactions of dimethyl- and diphenylgermylene ($GeMe_2$ and $GePh_2$, respectively) with cyclohexene oxide (CHO) and propylene sulfide (PrS) have been studied in hydrocarbon solvents at 25 °C by laser flash and steady-state photolysis methods using appropriately substituted germacyclopent-3-ene derivatives as germylene precursors. $GeMe_2$ reacts with CHO and PrS with rate constants in the range of 1.2–1.7 × 10^{10} M^{-1} s^{-1} in hexanes at 25 °C to form new transient products that are assigned to the corresponding Lewis acid-base complexes of the germylene with the substrates. The complexation reactions were found to be reversible and are characterized by equilibrium constants of K_C = (3.7 ± 0.8) × 10^3 M^{-1} and (3 ± 1) × 10^4 M^{-1} for complexation of $GeMe_2$ with CHO and PrS, respectively. The complexes decay over approximately 10 μs with the concomitant formation of tetramethyldigermene (Ge_2Me_4), identifiable by its characteristic UV-vis spectrum centered at λ_{max} = 370 nm. Diphenylgermylene behaves analogously, reacting rapidly and reversibly with the two substrates to form the corresponding Lewis acid-base complexes (λ_{max} ≈ 355 nm) that decay over several tens of microseconds with the concomitant growth of the characteristic UV-vis spectrum of tetraphenyldigermene (Ge_2Ph_4) (λ_{max} = 440 nm). Steady-state photolysis of the germylene precursors in the presence of CHO afforded germanium-containing oligomers but showed no evidence of oxygen abstraction or the formation of substrate-derived product(s). Similar photolyses in the presence of PrS also afforded germanium-containing oligomers, but as well yielded propene in 20%–30% yield and (in the case of the $GePh_2$ precursor) minor amounts of low molecular weight compounds that appear to be derived from the corresponding germanethione. Density functional theory calculations of the chalcogen abstraction reactions of $GeMe_2$ with oxirane and thiirane in the gas phase have been carried out at the B3LYP/6-311+G(d,p) level of theory and are in good qualitative agreement with the experimental data.

Key words: germylene, dimethylgermylene, diphenylgermylene, oxirane, thiirane, laser flash photolysis, chalcogen abstraction.

Résumé : Nous avons étudié les réactions du diméthyl- et du diphénylgermylène ($GeMe_2$ et $GePh_2$ respectivement) avec l'oxyde de cyclohexène (OCH) et le sulfure de propylène (PrS) dans des solvants hydrocarburés à 25 °C par les méthodes de photolyse éclair au laser et à l'état d'équilibre, en utilisant comme précurseurs germyléniques des dérivés de germacyclopent-3-ène adéquatement substitués. Le $GeMe_2$ réagit avec l'OCH et le PrS à des constantes de vitesse de l'ordre de 1,2 à 1,7 × 10^{10} M^{-1} s^{-1} dans l'hexane à 25 °C pour former de nouveaux produits intermédiaires que l'on attribue aux complexes acide-base de Lewis du germylène avec les substrats. Les réactions de complexation se sont révélées réversibles et sont caractérisées par des constantes d'équilibre K_C de (3,7 ± 0,8) × 10^3 M^{-1} et de (3 ± 1) × 10^4 M^{-1} correspondant à la complexation du $GeMe_2$ avec l'OCH et le PrS respectivement. Les complexes se dissocient en environ 10 μs, et on observe simultanément la formation de tétraméthyldigermène (Ge_2Me_4) identifiable par sa bande caractéristique en UV-vis centrée à λ_{max} = 370 nm. Le diphénylgermylène se comporte de façon analogue et réagit rapidement et de façon réversible avec les deux substrats pour former les complexes acide-base de Lewis correspondants (λ_{max} ≈ 355 nm) qui se dissocient sur une période de plusieurs dizaines de millisecondes, et on observe simultanément l'augmentation de l'intensité de la bande caractéristique en UV-vis du tétraphénylgermène (Ge_2Ph_4) (λ_{max} = 440 nm). La photolyse à l'état d'équilibre des précurseurs germyléniques en présence d'OCH a révélé la formation d'oligomères contenant du germanium, mais n'a indiqué aucun signe d'arrachement de l'atome d'oxygène ou de formation de produits dérivés des substrats. Des réactions similaires de photolyse en présence de PrS ont également produit des oligomères contenant du germanium, mais aussi du propène avec un rendement de 20% à 30% et (dans le cas du précurseur $GePh_2$) des composés de faible poids moléculaire en quantités minoritaires qui semblaient être dérivés de la germanethione correspondante. Des calculs théoriques de la fonctionnelle de la densité appliqués aux réactions d'arrachement du chalcogène de l'oxirane et du thiirane en phase gazeuse par le $GeMe_2$ ont été effectués au niveau B3LYP/6-311+G(d,p) de la théorie et concordent bien avec les données expérimentales sur le plan qualitatif. [Traduit par la Rédaction]

Mots-clés : germylène, diméthylgermylène, diphénylgermylène, oxirane, thiirane, photolyse éclair au laser, arrachement du chalcogène.

Received 7 September 2014. Accepted 9 October 2014.

S.S. Kostina and W.J. Leigh. Department of Chemistry and Chemical Biology, McMaster University, 1280 Main Street West, Hamilton, ON L8S 4M1, Canada.

Corresponding author: William J. Leigh (e-mail: leigh@mcmaster.ca).

This article is part of a Special Issue and is dedicated to our friend Stan Brown, with great respect and admiration.

Published at www.nrcresearchpress.com/cjc on 20 October 2014.

Introduction

Chalcogen abstraction reactions by silylenes and germylenes are amongst the most commonly used methods for the synthesis of compounds possessing tetrel–chalcogen double bonds. For example, stable silacarbonyl compounds have been synthesized by reactions of silylenes with N_2O,[1–6] CO_2,[1] O_2[1,7] and $H_2O{\cdot}B(C_6F_5)_3$,[8] whilst the first two stable germanones to be reported were prepared by reaction of sterically protected germylenes with trialkylamine *N*-oxides.[9,10] Stable silane- and germanethiones have also been prepared by abstraction reactions involving sterically encumbered or donor-stabilized tetrylenes, for example with phenyl isothiocyanate or styrene episulfide[11] as sulfur donors;[12] the desulfurization of sila- and germatetrathiolanes is another commonly used method for the preparation of stable M=S bond-containing compounds.[13–15]

Silanones are suspected intermediates in the reactions of transient silylenes with substrates such as N_2O,[16–21] CO_2,[22] aryl nitrile oxides,[23] aryl- and alkylisocyanates,[11] dialkylsulfoxides,[24–26] and oxiranes;[27–31] formal oxygen abstraction from oxiranes has also been found to proceed with transient germylenes in the presence of amines.[32–36] The only tetrylene-derived method for the formation of transient silane- and germanethiones that has been reported is sulfur abstraction from thiiranes.[31,34–37] With transient derivatives, the usual fate of the initially formed M=X-containing species is trimerization or (when prepared by abstraction from oxiranes or thiiranes) insertion into a second molecule of the substrate to form five-membered heterocycles.

Kinetic studies of the reactions of transient silylenes with oxiranes have been carried out in the gas phase[38] and in solution[31] and are supported by numerous theoretical studies.[31,39–41] The formation of silanethiones via sulfur abstraction from thiiranes has also been addressed computationally.[31,39,41] The reaction proceeds via the initial formation of the corresponding silylene–oxirane complex, of which several have been detected and characterized in solution.[31] This first stage of the reaction takes place with rate constants approaching the collisional limit in the gas phase for SiH_2 + oxirane[42] and at close to the diffusional rate for the reactions of $SiMe_2$ and $SiPh_2$ with propylene and cyclohexene oxide (PrO and CHO, respectively) in hexanes solution at 25 °C (i.e., $k \approx (1–2) \times 10^{10}$ M^{-1} s^{-1}).[31] The complexes, which exhibit UV-vis spectra typical of silylene–O–donor Lewis acid-base complexes,[43–45] are stabilized strongly enough relative to the free silylenes that they are formed as discrete, nonequilibrating intermediates in solution where they decay with clean first-order kinetics and rate constants in the $(3–4.5) \times 10^6$ s^{-1} range at 25 °C.[31] The dominant mode of decay is presumably via reaction to yield the corresponding silanone and alkene, which density functional theory (DFT) calculations suggest occurs via a stepwise mechanism involving a (singlet) 1,4-biradical intermediate.[31,41] The variations in the decay rate constants of the four silylene–oxirane complexes with substituent are not particularly large, but they are nevertheless consistent with the stepwise mechanism (eq. 1).

(1)

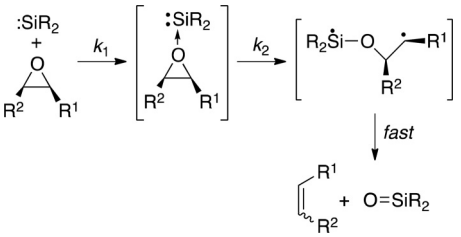

Sulfur abstraction from thiiranes has also been shown to proceed via the initial, diffusion-controlled formation of the corresponding silylene–thiirane Lewis acid-base complex.[31] The complexes of $SiMe_2$ and $SiPh_2$ with propylene sulfide (PrS) are significantly shorter lived than the corresponding complexes with PrO. Calculations for SiH_2 and $SiMe_2$ reproduce the higher reactivity of the thiirane system compared to the oxirane and predict that the complexes proceed to propene and the corresponding silanethione directly via a concerted two-bond cleavage mechanism.[31,39–41] The $SiPh_2$–PrS complex decays with a rate constant of approximately 2×10^7 s^{-1} (hexanes, 25 °C) to yield a new transient product that exhibits λ_{max} = 275 nm and has been assigned to diphenylsilanethione ($Ph_2Si{=}S$) based on its reactivity toward MeOH, ^{t}BuOH, AcOH, and $nBuNH_2$.[31]

Transient silanones and silanethiones generated by oxygen/sulfur abstraction from oxiranes and thiiranes by silylenes have been trapped by 1,1,3,3,5,5-hexamethylcyclotrisiloxane (D_3; eq. 2).[28,29,31]

(2)

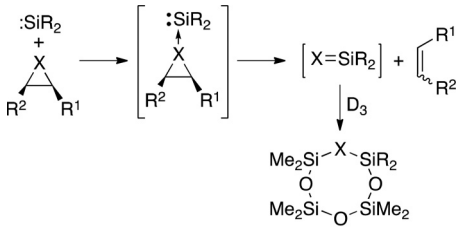

or MeOH,[31] the products of which are formed along with the corresponding alkenes in yields of 50%–70% relative to consumed silylene precursor. Transient silanones have also been shown to react with dienes[27] and oxiranes[30] to form stable products.

In this paper, the results of a laser flash photolysis study of the reactions of dimethyl- and diphenylgermylene ($GeMe_2$ and $GePh_2$, respectively) with CHO and PrS in hexanes solution are presented. The goals of the study were to compare the kinetic and spectroscopic behaviors of $GeMe_2$ and $GePh_2$ in the presence of these substrates to those of the corresponding silylenes to see whether any indication of reaction could be obtained, and if so, to determine the course of reaction and obtain kinetic and (or) thermodynamic details relating to the mechanism(s). The laser photolysis studies are supplemented with product studies of the reactions of the two species with CHO and PrS in cyclohexane-d_{12} solution. We also carried out DFT calculations of the reactions of $GeMe_2$ with oxirane and thiirane and compare the results to the experimental data for $GeMe_2$ and to earlier DFT calculations on the analogous reactions of the silicon homolog ($SiMe_2$).[31]

Results

The two transient germylenes were generated by laser photolysis of rapidly flowed, deoxygenated hexanes solutions of the germacyclopent-3-enes **1a**, **1b**, and **2**, respectively, using a KrF excimer laser (248 nm, 90–105 mJ, approximately 25 ns) for excitation and time-resolved UV-vis spectroscopy to monitor the germylenes and their reaction products. Laser photolysis of these compounds leads to the prompt formation of readily detectable transient absorptions centered at λ_{max} = 470 nm[46,47] for $GeMe_2$ and λ_{max} = 300 and 500 nm[48] in the case of $GePh_2$, which decay on the microsecond timescale with second-order kinetics to yield the corresponding digermenes Ge_2Me_4 (Me_2Ge = $GeMe_2$, λ_{max} = 370 nm)[46–48] and Ge_2Ph_4 (Ph_2Ge = $GePh_2$; λ_{max} = 440 nm),[48] respectively. As reported previously,[46] the $GeMe_2$ precursors **1a** and **1b** afford very similar time-resolved spectroscopic behavior, the only real difference being that **1a** gives rise to somewhat stronger transient absorptions than **1b** (all else being equal) owing to a larger quantum yield for reaction. In the experiments with the $GePh_2$ precursor (**2**), the rate coefficients for decay of the germylene were determined using absorbance–time data recorded at 500 nm, corrected for the underlying contribution of the digermene absorption at this wavelength following the protocol established in earlier work.[48,49]

Fig. 1. Absorbance–time profiles for $GeMe_2$ in deoxygenated hexanes containing (*a*) 0 and 0.5 mmol L^{-1} CHO and (*b*) 0 and 0.2 mmol L^{-1} PrS at 25 °C. The data were recorded at a monitoring wavelength of 470 nm using **1a** as precursor for the experiments with CHO and **1b** for those with PrS.

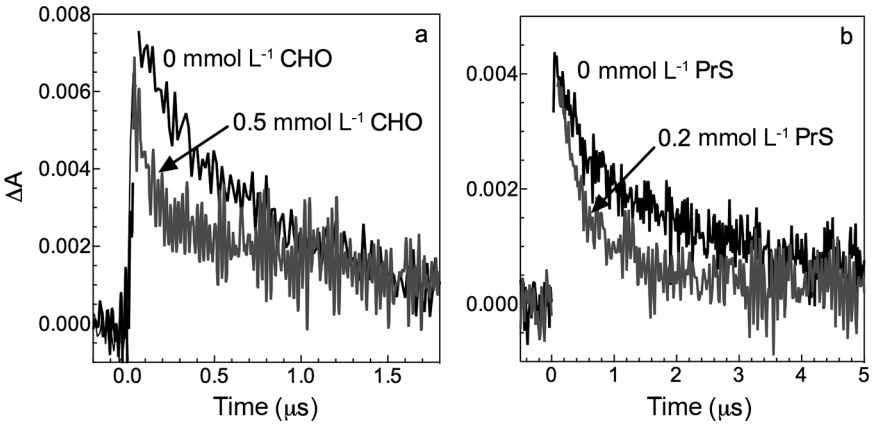

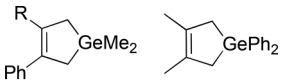

1 **2**

1a. R = H
1b. R = Me

In the presence of submillimolar concentrations of CHO or PrS, transient decays recorded for $GeMe_2$ were bimodal, consisting of a rapid initial decay component and a slowly decaying residual absorbance. The initial decay became more rapid and the intensity of the residual absorbance was reduced as the substrate concentration was increased (Fig. 1), behavior that is consistent with a reversible reaction characterized by an equilibrium constant in the approximate range of $1 \times 10^3\ M^{-1} < K_C < 3 \times 10^4\ M^{-1}$.[45,50] The fast initial decay is the (pseudo-first-order) approach to equilibrium; the kinetics are described (approximately) by eqs. 3 and 4:

$$\Delta A_t = \Delta A_{res} + (\Delta A_0 - \Delta A_{res}) \exp(-k_{decay} t) \quad (3)$$

$$k_{decay} = k_{-C} + k_C[Q] \quad (4)$$

where ΔA_0, ΔA_t, and ΔA_{res} are the values of the germylene transient absorbance immediately after the laser pulse, at time t after the pulse, and at the end of the initial decay, respectively, k_{decay} is the pseudo-first-order rate coefficient for decay of the germylene, and k_C and k_{-C} are the forward and reverse rate constants for reaction with the substrate (Q). The slow decay of the residual absorption is due to dimerization of the germylene, in equilibrium with the product of the reversible germylene–substrate reaction. Its detection allows for the equilibrium constant ($K_C = k_C/k_{-C}$) to be determined from analysis of the data according to eq. 5:

$$(\Delta A_0)_0/(\Delta A_{res})_Q = 1 + K_C[Q] \quad (5)$$

where $(\Delta A_0)_0$ is the ΔA_0 value due to the germylene in the absence of substrate and $(\Delta A_{res})_Q$ is the value of ΔA_{res} in the presence of a given concentration of substrate Q; the latter was typically estimated by visual inspection of the decay profile (as the breakpoint in the bimodal decay). The forward rate constants were estimated from plots of k_{decay} versus [CHO] or [PrS], which displayed good linearity in both cases (see Fig. 2*a*); analysis of the data according to eq. 4 yielded rate constants of $k_C = (1.2 \pm 0.3) \times 10^{10}\ M^{-1}\ s^{-1}$ and $k_C = (1.7 \pm 0.2) \times 10^{10}\ M^{-1}\ s^{-1}$ for the reactions with CHO and PrS, respectively. The plots of $(\Delta A_0)_0/(\Delta A_{res})_Q$ versus [PrS] and [CHO] were also linear in both cases (see Fig. 2*b*), and regression analysis afforded equilibrium constants of $K_C = (3 \pm 1) \times 10^4\ M^{-1}$ and $K_C = (3.7 \pm 0.8) \times 10^3\ M^{-1}$, respectively. As will be shown below, the products of these reversible reactions are the corresponding germylene–substrate Lewis acid-base complexes.

Bimodal decay kinetics were also observed of the (corrected) germylene absorbance–time profiles obtained from solutions of **2** in hexanes containing submillimolar concentrations of CHO, which is again consistent with reversible reaction between the germylene and the substrate. Analysis of the data according to eqs. 4 and 5 afforded rate and equilibrium constants of $k_C = (8 \pm 1) \times 10^9\ M^{-1}\ s^{-1}$ and $K_C = (2.4 \pm 0.5) \times 10^4\ M^{-1}$, respectively (Fig. S1) (see Supplementary material section). In contrast, addition of PrS to a hexanes solution of **2** caused the (corrected) germylene absorption to decay with clean first-order kinetics completely to baseline at even the lowest concentration studied (0.1 mmol L^{-1}). A plot of k_{decay} versus [PrS] yielded a straight line with a slope of $k_C = (8 \pm 2) \times 10^9\ M^{-1}\ s^{-1}$.

Transient absorption spectra were recorded with solutions of **1a** and **2** in hexanes containing either PrS (approximately 5 mmol L^{-1}) or CHO (10–50 mmol L^{-1}). New promptly formed transient absorptions were observed in all four cases, which were centered in the 270–310 nm range for the $GeMe_2$-derived species (see Fig. 3) and at $\lambda_{max} \approx 355$ nm for the $GePh_2$-derived ones (Fig. S2). The absorptions decay over several tens of microseconds with second-order decay kinetics with the concomitant growth of longer-wavelength absorption bands due to the corresponding digermenes (Ge_2Me_4 and Ge_2Ph_4). The spectra and kinetic behavior are quite similar to those reported previously for the Lewis acid-base complexes of the two germylenes with tetrahydrofuran (THF) and tetrahydrothiophene (THT) under similar experimental conditions[45,51] and are thus assigned to the corresponding Lewis acid-base complexes with CHO and PrS. In addition to the signals due to the $GePh_2$–CHO complex and Ge_2Ph_4, another even longer-lived product ($\lambda_{max} \leq 280$ nm) was also detected, its growth kinetics indicating that it is most likely associated with a higher $GePh_2$ oligomer. A long-lived transient with similar characteristics was also evident in the transient spectra from a solution of **2** in hexanes containing 5 mmol L^{-1} PrS, although the signal was less intense (Fig. S2).

Time-resolved UV-vis spectra were also recorded with hexanes solutions of **1a** and **2** containing approximately 5 mmol L^{-1} diethyl sulfide (Et_2S) for comparison to the spectra of the complexes of the two germylenes with thiirane and THT[45] and to see whether similar long-lived product absorptions are obtained in the presence of the acyclic dialkyl sulfide as with the cyclic ones. The addition of submillimolar concentrations of Et_2S to the solutions caused the germylene absorptions to decay completely to prepulse levels with clean first-order decay kinetics; complexation

Fig. 2. Plots of (*a*) k_{decay} versus [Q] and (*b*) $(\Delta A_0)_0/(\Delta A_{res})_Q$ versus [Q] for $GeMe_2$ in deoxygenated hexanes containing varying concentrations of CHO (●) and PrS (○) at 25 °C; the solid lines are the linear least-squares fits of the data to to eqs. 4 (Fig. 2*a*) and 5 (Fig. 2*b*). Absorbance–time profiles were recorded at 470 nm using **1a** as the precursor for experiments with CHO and **1b** for those with PrS.

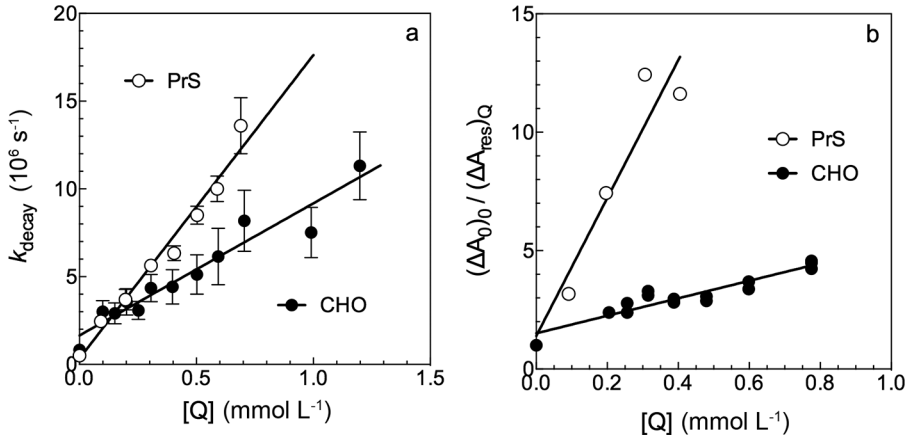

Fig. 3. (*a*) Transient absorption spectra recorded 0.16–0.80 μs (○) and 4.96–5.60 μs (□) after the laser pulse by laser photolysis of **1a** in deoxygenated hexanes containing 0.05 mol L^{-1} CHO at 25 °C; (*b*) Transient absorption spectra recorded 0.00–0.64 μs (○) and 5.60–6.24 μs (□) after the laser pulse, from a similar experiment with **1a** in deoxygenated hexanes containing 0.005 mol L^{-1} PrS. The insets show transient decay traces recorded at 310 and 370 nm.

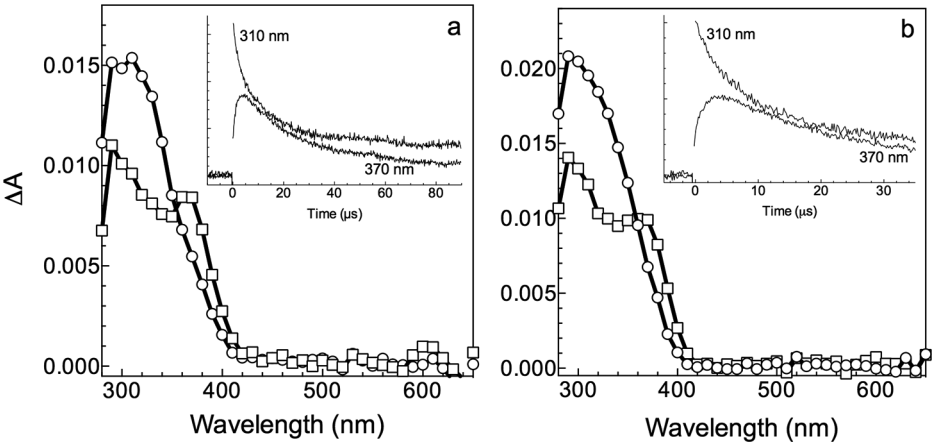

rate constants of k_C = (1.8 ± 0.2) × 10^{10} M^{-1} s^{-1} and (8.3 ± 0.4) × 10^9 M^{-1} s^{-1} were obtained from the slopes of (linear) plots of k_{decay} versus [Et_2S] for $GeMe_2$ and $GePh_2$, respectively (Fig. S3*a*). Transient absorption spectra in the presence of 5 mmol L^{-1} Et_2S (Figs. S3*b*, and S3*c*) show absorptions centered at λ_{max} = 300 and 345 nm, respectively, which are assigned to the corresponding complexes. The data for the $GePh_2$–Et_2S system reveal a long-lived absorption below 300 nm that grows in on a similar timescale as the decay of the digermene, analogous to the behavior observed for the $GePh_2$–PrS system.

Table 1 lists the rate and (or) equilibrium constants determined in this work for the complexation of $GeMe_2$ and $GePh_2$ with CHO, PrS, and Et_2S in hexanes at 25 °C and the UV-vis absorption maxima of the corresponding complexes. The table also contains the corresponding kinetic and spectroscopic data for complexation of the two germylenes with Et_2O, THF, and THT under similar conditions to emphasize the similarities between the behaviors of the two species with CHO and PrS and with the larger ring cyclic ether and sulfide.

Product studies

Initial steady-state photolysis experiments were carried out on deoxygenated 0.05 mol L^{-1} solutions of **1b** in cyclohexane-d_{12} containing CHO or PrS (approximately 0.2 mol L^{-1}) and Si_2Me_6 (0.01 mol L^{-1}) as internal integration standard, monitoring the course of 254 nm photolysis by ^1H NMR spectroscopy (Figs. S4 and S6). Both product mixtures appeared to be quite complicated, the spectra showing complex collections of signals in the δ 0.3–0.6 range of the spectrum that are indicative of the formation of several germanium-containing products, in addition to the characteristic resonances due to diene **3**. Cyclohexene was not formed in detectable amounts in the photolysis with CHO (eq. 6), but propene (**4**) could be conclusively identified in the PrS-containing photolysate (eq. 7):

(6)

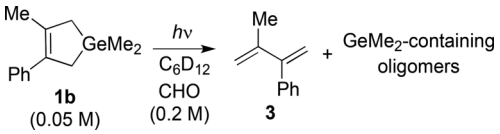

(7)

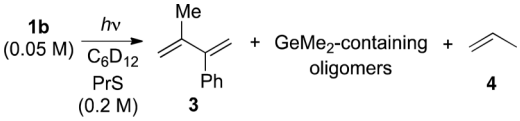

Concentration versus time plots constructed for **3** and the two substrates (Figs. S5 and S7) indicate the rates of substrate consumption to be similar to (in the case of CHO) or higher than (in

Table 1. Bimolecular rate and equilibrium constants and free energies[a] for complexation of $GeMe_2$ and $GePh_2$ with oxygen and sulfur donors in hexanes at 25 °C and UV-vis absorption maxima of the corresponding complexes, also in hexanes at 25 °C.

System	k_C (10^{10} M^{-1} s^{-1})	K_C (10^3 M^{-1})	ΔG (kcal mol^{-1})	λ_{max} (nm)[a]
$GeMe_2$–CHO	1.2±0.3	3.7±0.8	–3.0±0.1	≤300[b]
$GeMe_2$–THF	1.1±0.2[b]	10±4[b]	–3.5±0.3	310[b]
$GeMe_2$–Et_2O	—[c,d]	0.11±0.01[d]	–0.9±0.1	300[d]
$GeMe_2$–PrS	1.7±0.2	30±10	–4.2±0.2	≤300[b]
$GeMe_2$–THT	1.7±0.2[d]	>30[d]	<–4.1	320[d]
$GeMe_2$–Et_2S	1.8±0.2	>30	<–4.1	300[a]
$GePh_2$–CHO	0.8±0.1	24±5	–4.1±0.1	355[a]
$GePh_2$–THF	0.63±0.06[b]	23±5[b]	–4.0±0.1	360[b]
$GePh_2$–Et_2O	—[c,d]	0.16±0.01[d]	–1.1±0.1[d]	360[d]
$GePh_2$–PrS	0.8±0.2	>30	<–4.1	355[a]
$GePh_2$–THT	1.0±0.2[d]	>30[d]	<–4.1	350[d]
$GePh_2$–Et_2S	0.83±0.04	>30	<–4.1	350[a]

[a]Standard state is the gas phase at 1 atm pressure and 298.15 K; calculated from the solution phase equilibrium constants or the lower limit.
[b]Leigh et al.[50]
[c]k_C indeterminable.
[d]Kostina et al.[45]

the case of PrS) the rate of diene formation. The NMR spectra of the photolysed mixtures, the CHO photolysate in particular, also showed broad baseline absorptions, consistent with polymer formation. Compound **1b** could not be quantified in these experiments because of spectral overlap between its NMR resonances and those due to photoproducts, and thus, product yields relative to consumed germylene precursor could not be determined. Nevertheless, propene (**4**) was formed at roughly one third of the rate of diene **3** in the photolysis with PrS as substrate over the photolysis period monitored.

The reaction with PrS was repeated using **1a** as $GeMe_2$ precursor, as this compound's vinylic hydrogen provides a well-separated signal in the NMR spectrum to allow quantitation throughout the photolysis. Irradiation of a C_6D_{12} solution of **1a** (0.047 mol L^{-1}) containing PrS (0.07 mol L^{-1}) and Si_2Me_6 (0.012 mol L^{-1}) for 15 min (approximately 17% conversion of **1a**; Fig. S8) resulted in the formation of diene **5** and propene (**4**) in yields of 70% and 20% relative to consumed **1a**, respectively (eq. 8), based on the relative slopes of concentration versus time plots (Fig. S9):

(8)

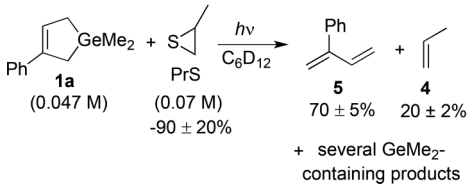

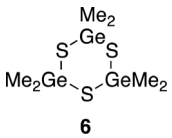

6

A spiking experiment in which a small quantity of an authentic sample of the anticipated oligomerization product of dimethylgermanethione, cyclic trimer **6**,[34–36] showed that this compound was *not* present in the photolysis mixture after 15 min of irradiation (Fig. S10). GC/MS analysis of the photolysate verified the presence of **5** as the major photoproduct and also showed at least eight additional products formed in minor amounts. The mass spectra (Fig. S11) indicated that seven of these contained at least two germanium atoms, while the remaining one contained none. The seven germanium-containing compounds share the same fragment with m/z = 119, which is consistent with a $GeMe_3^+$ unit. Unfortunately, none of these compounds could be identified conclusively.

Similar results were obtained in steady-state photolysis experiments carried out with cyclohexane-d_{12} solutions of **2** (approximately 0.06 mol L^{-1}) in the presence of CHO (0.085 mol L^{-1}) or PrS (0.08 mol L^{-1}); these experiments were carried out in parallel with a third one in which a 0.05 mol L^{-1} solution of **2** in cyclohexane-d_{12} was irradiated in the absence of an added substrate. All three photolyses produced 2,3-dimethyl-1,3-butadiene (**7**) as the major identifiable product, along with (presumably oligomeric) materials giving rise to broad, ill-defined resonances in the δ 6.7–7.7 and 0.5–2.5 regions of the spectrum (Figs. S12 and S14). No consumption of CHO was evident in the experiment with that substrate after approximately 17% of conversion of **2** (Fig. S13), and no cyclohexene was formed in detectable amounts (Fig. S12). On the other hand, photolysis of **2** in the presence of PrS resulted in the formation of **7** and **4** in approximate yields of 80% and 32%, respectively, relative to consumed **2** (eq. 9; Fig. S15):

(9)

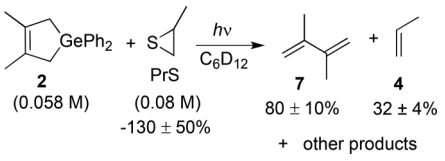

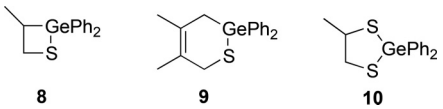

The rates of consumption of PrS and **2** were approximately equal. Removal of the volatile components of the PrS-photolysate and redissolution of the residue in C_6D_{12} resulted in an NMR spectrum that showed four weak but well-defined multiplets in the δ 7.5–7.9 region of the spectrum, superimposed on broad baseline absorptions due (presumably) to oligomeric materials. GC/MS analysis of the mixture indicated the presence of three new compounds in minor amounts, the mass spectra of which are consistent with 1:1 adducts of $GePh_2$ and PrS (e.g., **8**), $Ph_2Ge{=}S$ and DMB (e.g., **9**), and $Ph_2Ge{=}S$ and PrS (e.g., **10**). Products of this type all have precedence from early studies of the reactions of so-called

Fig. 4. Calculated (B3LYP/6-311+G(d,p)) structures and selected bond distances (in Å) and angles (in degrees) of the $GeMe_2$–oxirane and $GeMe_2$–thiirane complexes ("C_X"), the transition states for C–X bond cleavage ("TS_X"), and the first-formed products of the reaction; "β" denotes the C3–Ge–X–C2 dihedral angle (X = O or S). The methyl hydrogens have been omitted from the structures for clarity.

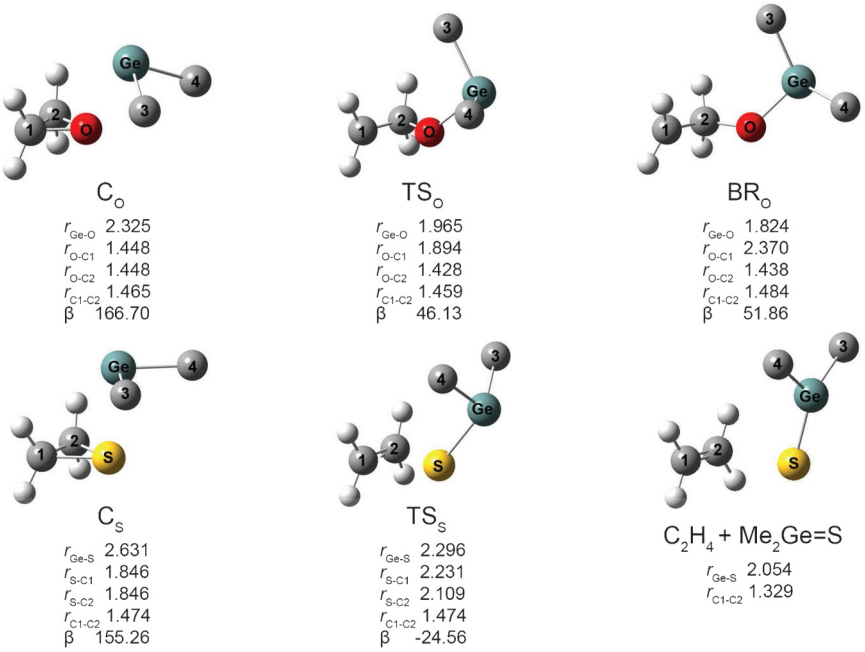

"germylene–amine complexes" with thiiranes under thermolytic conditions.[34–36]

Computational studies

Thermochemical parameters for the formation of the complexes of $GeMe_2$ with oxirane and thiirane and of the first step in the transfer of the chalcogen atom to germanium were modeled using DFT employing the B3LYP hybrid exchange-correlation functional[52,53] in conjunction with the 6-311+G(d,p) basis set. This is the same level of theory as was used in our earlier study of the reactions of $SiMe_2$ with these substrates to allow direct comparisons.[31] Starting structures for geometry optimization of the complexes and the transition states for their decomposition were constructed from the homologous structures from our earlier study, applying reasonable adjustments to bond distances and angles involving the heavy group 14 element to account for the substitution of silicon with germanium.[45] The transition states were optimized using the unrestricted procedure with HOMO–LUMO mixing in the initial guess leading to unrestricted wave functions and were confirmed to be first-order saddle points on the basis of their vibrational frequencies. Intrinsic reaction coordinate calculations starting at the saddle points were carried out in the reverse direction to verify the connection with the complexes and in the forward direction to establish starting structures for the final geometry optimizations of the primary decomposition products. The intrinsic reaction coordinate calculations were also carried out using the unrestricted procedure with HOMO–LUMO mixing, as were the final geometry optimizations and frequency calculations for the biradical intermediate found in the $GeMe_2$ plus oxirane reaction system (*vide infra*). The reported thermodynamic data (*vide infra*) were computed at 298.15 K from unscaled vibrational frequencies.

Figure 4 shows the calculated (B3LYP/6-311+G(d,p)) structures of the Lewis acid-base complexes of $GeMe_2$ with oxirane and thiirane (C_X, X = O or S), the transition states for C–X bond cleavage in the complexes (TS_X), and the primary products of the reactions: the $Me_2GeOCH_2CH_2$ biradical from the $GeMe_2$–oxirane complex (BR_O) and ethylene and dimethylgermanethione from the $GeMe_2$–thiirane complex. The two reaction systems both behave analogously to the corresponding SiH_2 and $SiMe_2$ systems.[31,41] Only the anti-conformer of each of the complexes was located; relaxed scans in which the C3–Ge–X–C2 dihedral angle was driven in 10° steps confirmed the anti-conformer to be the only minimum-energy conformer at this level of theory in both cases. Table 2 lists the B3LYP/6-311+G(d,p) electronic energies, standard enthalpies, and free energies of the various species investigated relative to those of the isolated germylene and substrate. The two most likely decomposition products of the $Me_2GeOCH_2CH_2$ biradical (Me_2Ge=O plus C_2H_4 and 1,1-dimethylgerma-2-oxetane) were also modeled, but the more complex task of locating transition states for the formation of these products from the biradical was not attempted.

Figure 5*a* summarizes the results of the B3LYP/6-311+G(d,p) calculations for the $GeMe_2$–oxirane and $GeMe_2$–thiirane systems as free energy reaction coordinate diagrams. Included for comparison is the analogous set of diagrams for the corresponding $SiMe_2$–oxirane and $SiMe_2$–thiirane systems at the same level of theory, from our earlier study.[31]

Discussion

The present work represents the first experimental study to be reported of the reactivity of simple, transient dialkyl- and diarylgermylenes with oxiranes and thiiranes under neutral ambient conditions, conditions under which the corresponding silylene derivatives react rapidly via formal oxygen or sulfur abstraction to afford the corresponding alkene and silanone[27–31,38] or silanethione,[31] respectively, in good chemical yields. The only related existing studies of the reactivity of Ge(II) systems with substrates of this type are those of Satgé and co-workers, who examined the reactions of a series of amine-coordinated germylenoids with oxiranes and thiirane.[32–35] Their experiments with these compounds, the crystalline products of reaction of Et_2GeHCl, PhMeGeHCl, and Ph_2GeHCl with pyridine/triethylamine in pentane (and formulated as the corresponding germylene-triethylamine

Table 2. Electronic energies (ΔE_{elec}), zero-point-corrected electronic energies (at 0 K, ΔE_0), standard enthalpies ($\Delta H°$), and free energies ($\Delta G°$) of stationary points on the potential energy surfaces for reaction of $GeMe_2$ with oxirane and thiirane, in kcal mol^{-1} relative to the energies of the free reactants, calculated at the B3LYP/6-311+G(d,p) level of theory.

	$GeMe_2$ + oxirane (X = O)				$GeMe_2$ + thiirane (X = S)			
	ΔE_{elec}	ΔE_0	$\Delta H°$	$\Delta G°$	ΔE_{elec}	ΔE_0	$\Delta H°$	$\Delta G°$
anti-Complex (C_X)	–9.3	–7.7	–7.6	+2.7	–11.3	–9.6	–9.6	+1.2
Transition state (TS_X)	+7.4	+7.5	+7.4	+18.9	+0.5	+0.9	+1.1	+11.8
Biradical (BR)	–3.6	–3.6	–3.2	+6.6	—	—	—	—
$R_2Ge{=}X + C_2H_4$	–26.5	–27.5	–26.9	–27.7	–34.8	–34.9	–34.3	–35.0

Fig. 5. Free energy reaction coordinate diagrams for the oxygen and sulfur abstraction reactions of (*a*) $GeMe_2$ and (*b*) $SiMe_2$ with oxirane and thiirane calculated at the B3LYP/6-311+G(d,p) level of theory.

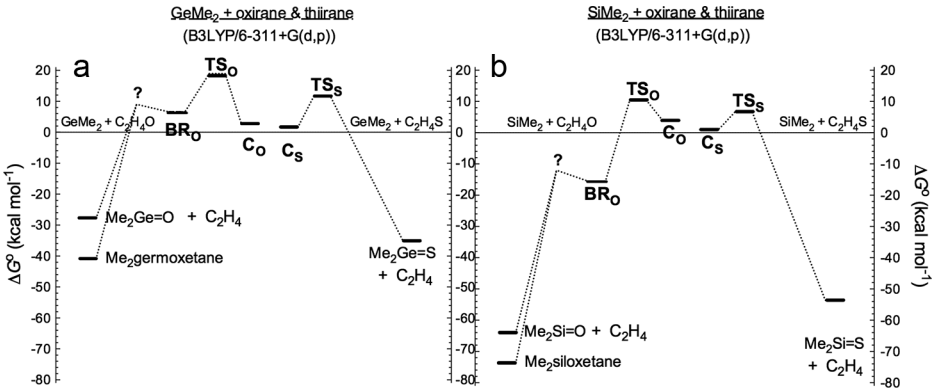

complexes **11** (eq. 10))[54] involved thermolysing the materials with 2–3 equiv. of substrate in sealed tubes at 130–150 °C:

(10) 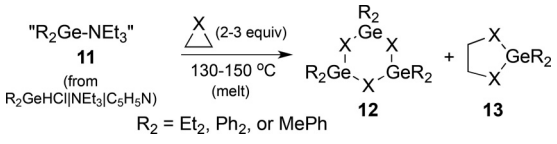

This typically afforded mixtures of the corresponding ($R_2Ge{=}X$) trimer (**12**) and the (2+3)-cycloadduct of $R_2Ge{=}X$ with a second molecule of substrate (**13**; eq. 10).[32–35] The formation of $R_2Ge{=}X$ was proposed to occur via elimination of ethylene from a germoxetane or thietane intermediate derived from insertion of GeR_2 into a C–X bond of the substrate:

(11) 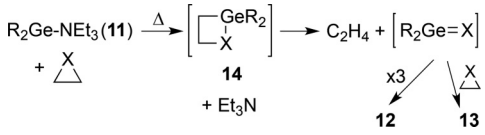

The high temperatures required for these reactions are undoubtedly needed, at least in part, because of the presence of the amine, which binds to the free germylene many orders of magnitude more strongly than oxygen or sulfur donors[45] and (presumably) must be disengaged from the Ge(II) species in order for reaction to occur. As well, the barrier(s) to reaction of the free germylenes are significantly higher than in the silicon systems,[21,55,56] which may also contribute to the need for rather severe conditions to effect reaction.

The results of our experiments indicate that at room temperature in hydrocarbon solvents, neither $GeMe_2$ nor $GePh_2$ abstracts oxygen from the representative oxirane derivative CHO with an overall rate constant large enough to compete with the germylene oligomerization processes that occur in the absence of reactive substrates.[45–48,50] The laser photolysis experiments provide clear evidence of a rapid, nearly diffusion-controlled reaction between the two germylenes and the substrate to afford the corresponding Lewis acid-base complexes, which appear to be virtually inert to further (unimolecular) reaction; they exist in equilibrium with the free germylenes and the substrate and appear to play no role in the chemistry other than mediating germylene dimerization and the formation of higher oligomers. The complexes exhibit nearly identical UV-vis spectra and kinetic behavior to those of the complexes of $GeMe_2$ and $GePh_2$ with less potentially reactive oxygen donors such as THF and Et_2O (see Table 1).[45,50,57] The equilibrium constants for complexation of $GeMe_2$ and $GePh_2$ with CHO are similar to or slightly smaller than those with THF in each case (and much larger than those with Et_2O) and indicate binding free energies of $\Delta G \approx -3.0$ and -4.1 kcal mol^{-1}, respectively (Table 1), where the standard state has been converted to the gas phase at 1 atm and 298.15 K. The larger K_C value exhibited by $GePh_2$ compared to $GeMe_2$ is also observed for complexation of the two species with Et_2O and THF under similar conditions and reflects the enhancement in germylene Lewis acidity that results from phenyl-for-methyl substitution at the Ge(II) center.[45]

On the other hand, generation of the two species in the presence of approximately 0.1 mol L^{-1} PrS under lamp photolysis conditions affords propene in yields of 20%–30%, indicating significantly greater reactivity with this substrate than with the oxirane derivative. However, reaction with the substrate is still inefficient compared to oligomerization, even at the extremely low steady-state transient concentrations that characterize our lamp photolysis experiments. This means that under the conditions of our laser photolysis experiments, where micromolar concentrations of germylene are produced within the approximately 25 ns laser pulse, dimerization should be the only reaction pathway accessible. Indeed, the time-resolved behavior of the two species in the presence of PrS shows evidence only of Lewis acid-base complexation and the formation of the corresponding digermenes and higher oligomers absorbing below 300 nm (see Scheme 1). The $GeMe_2$–PrS and $GePh_2$–PrS complexes exhibit UV-vis absorption

Scheme 1.

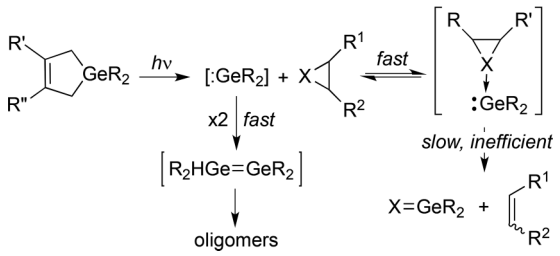

maxima of λ_{max} = 300 and 345 nm, respectively, similar to the spectra of the corresponding germylene–THT[45] and germylene–Et_2S complexes under the same conditions. The kinetic data are consistent with an estimated upper limit of approximately 10^4 s^{-1} for the unimolecular rate constant for the second step in the sulfur abstraction process (i.e., collapse of the complexes to products), which corresponds to a reaction free energy barrier of approximately 12 kcal mol^{-1} or greater. The response of the germylene absorbance–time profiles to added PrS (*vide supra*) is consistent with binding free energies of approximately 4.2 kcal mol^{-1} (for $GeMe_2$) or greater (for $GePh_2$), where the reference state is again the gas phase at 1 atm and 298.15 K. The higher binding energies for the complexes with PrS compared to CHO is also consistent with previous observations for other oxygen and sulfur donors of homologous structures.[45]

The DFT calculations, which focus on the first steps in the oxygen and sulfur abstraction reactions of $GeMe_2$ with oxirane and thiirane, respectively, were carried out at the same level of theory as was used in our earlier study of the reactions of $SiMe_2$ with these two substrates to enable direct comparisons. Figure 5 shows the calculated free energy reaction coordinate diagrams for the reactions of oxirane and thiirane with $GeMe_2$ (Fig. 5*a*) and $SiMe_2$ (Fig. 5*b*), the latter constructed from the data reported in our earlier study.[31] As expected,[40,58–62] the calculations for the Si(II) and Ge(II) systems are closely analogous to one another, the main differences being the higher reaction barriers and lower product stabilities for the Ge(II) systems than were found for the corresponding Si(II) ones. The calculations predict Lewis acid-base complexation to be the first step in all cases and that the reaction of a given tetrylene with thiirane should be significantly faster than that with oxirane, in good qualitative agreement with the experimental data. Comparison of the calculated binding free energies of the complexes to the corresponding experimental values, calculated from the measured equilibrium constants or their lower limits (Table 1), indicates that the calculations underestimate the stabilities of the intermediate complexes relative to the isolated reactants by about 5 kcal mol^{-1} in free energy; they do, however, correctly predict that the sulfur donor complexes enjoy slightly greater stability relative to the free tetrylene and substrate than the corresponding oxygen donor complexes for both of the tetrylene systems. For both $SiMe_2$ and $GeMe_2$, chalcogen abstraction is predicted to proceed via different mechanisms depending on the identity of the substrate, the MMe_2–oxirane complexes reacting via a nonconcerted mechanism involving cleavage of a single O–C bond in the first step to afford the corresponding $Me_2MOCH_2CH_2$ biradical, whilst C–S bond cleavage in the MMe_2-thiirane system is predicted to proceed concertedly to form $Me_2M{=}S$ and ethylene directly. Testing the validity of these mechanistic predictions, for the reactions of both silylenes and germylenes with oxiranes and thiiranes, is the subject of future work.

Summary and conclusions

The transient germylenes $GeMe_2$ and $GePh_2$ react with CHO and PrS reversibly to form the corresponding Lewis acid-base complexes, which have been detected and characterized in all four cases by laser flash photolysis. Under the conditions of the laser photolysis experiments, the complexes decay over several tens of microseconds with second-order kinetics to generate the corresponding digermenes as the only detectable mode of decay. No first-order decay component could be detected in the transient absorbance–time profiles due to the germylene–CHO and germylene–PrS complexes, from which it is concluded that unimolecular X–C bond cleavage in the complexes is too slow to compete with germylene dimerization at room temperature under the conditions of pulsed laser excitation. Steady-state photolysis experiments verify the absence of reactivity of the two germylenes with CHO but indicate that formal sulfur abstraction from PrS, leading to the formation of propene, proceeds in low (approximately 20%–30%) chemical yield from both transient germylenes in solution at ambient temperatures and is only modestly competitive with oligomerization under these conditions.

DFT calculations of the complexation of $GeMe_2$ with oxirane and thiirane in the gas phase and of the first step in the oxygen and sulfur abstraction reactions within the complexes have been carried out at the B3LYP/6-311+G(d,p) level of theory. The calculations underestimate the stabilities of the complexes by approximately 5 kcal mol^{-1} based on comparisons to the experimentally determined equilibrium constants for complexation of the two germylenes with CHO in hexanes at 25 °C, but they nevertheless correctly reproduce the ordering of stabilities found experimentally, and also the relative reactivities of the $GeMe_2$-PrS and $GeMe_2$-CHO complexes with respect to C–O and C–S bond cleavage, leading ultimately to the corresponding transient germanone and germanethione.

Further kinetic and mechanistic studies of the chemistry of transient heavy group 14 carbene analogs are in progress.

Experimental

^{1}H NMR spectra were recorded on Bruker AV500 or AV600 spectrometers in cyclohexane-d_{12} and were referenced to the residual solvent proton. GC/MS analyses were carried out on a Varian Saturn 2200 GC/MS/MS system equipped with a VF-5 ms capillary column (30 m × 0.25 mm, 0.25 μm) (Varian, Inc.). High-resolution electron impact mass spectra and exact masses were determined on a Micromass TofSpec 2E mass spectrometer using electron impact ionization (25 eV).

PrS, Et_2S, and CHO were purchased from Sigma-Aldrich and purified by distillation from anhydrous sodium sulphate (PrS and Et_2S) or CaH_2 (CHO). THF (Caledon Reagent) was refluxed over calcium hydride for 2 h, distilled into a flask containing sodium, and refluxed further for several days and then finally distilled under nitrogen. Hexanes (EMD OmniSolv) were dried by passage through activated alumina under nitrogen using a Solv-Tek solvent purification system (Solv-Tek, Inc.).

The germacyclopentene derivative **1b** was prepared following the reported procedure.[46] It was purified by column chromatography on silica gel using hexanes as eluent, which afforded the compound in >98% purity as determined by GC/MS. Compound **1a** was available from an earlier study.[45] Compound **2** was synthesized via the two-step procedure reported previously[48] and was purified by silica gel chromatography with hexanes as eluent followed by multiple recrystallizations from hexanes to remove traces of biphenyl.

Hexamethylcyclotrigermathiane (**6**) was prepared from lithium sulfide and dimethyl germanium dichloride using an adaptation of the method of Herzog and Rheinwald.[63] Li_2S was prepared by treating lithium (0.38 g of a 30% dispersion in mineral oil, 13.7 mmol) with elemental sulfur (0.19 g, 5.8 mmol) in dry THF (approximately 2 mL) under N_2. Refluxing for 12 h yielded a black solution to which was added a solution of Me_2GeCl_2 (1.01 g, 5.8 mmol) in THF (2.5 mL, distilled from $LiAlH_4$) dropwise via a

plastic syringe. The resulting tan solution was then stirred for 4 days at room temperature. The solvent was removed under high vacuum and 10 mL of benzene was added to yield a brown suspension, which was filtered by gravity filtration. An additional 15–20 mL of hexane was added to the benzene solution and the mixture was filtered. Evaporation of the solvent yielded the crude product as a green oil (0.50 g, 64% yield), which was distilled under vacuum to afford a yellow oil (bp = 83–84 °C, 0.05 mm Hg) that solidified to an oily solid upon standing at room temperature. The product was identified on the basis of its ^{1}H NMR (δ ($CDCl_3$) 0.98 (s)), ^{13}C NMR (δ ($CDCl_3$) 10.6), and GC/MS spectra.[63] Although the ^{1}H NMR spectra of the product indicated the presence of some impurities in the sample, further purification by column chromatography was not carried out.

Laser flash photolysis experiments were carried out using a Lambda Physik Compex 120 excimer laser filled with F_2/Kr/Ne (248 nm, 25 ns, 98–110 mJ pulse^{-1}) and a Luzchem Research mLFP-111 laser flash photolysis system, modified as described previously.[48] The solutions were prepared in deoxygenated anhydrous hexanes such that the absorbance at 248 nm was between 0.4 and 0.7. The solutions were flowed rapidly through a 7 mm × 7 mm Suprasil flow cell connected to calibrated 100 or 250 mL reservoirs, which contain a glass frit to allow bubbling of argon gas through the solution for 40 min prior to and throughout the experiment. The flow cell was connected to a Masterflex™ 77390 peristaltic pump fitted with Teflon tubing (Cole-Parmer Instrument Co.), which pulls the solution through the cell at a constant rate of 2–3 mL min^{-1}. The glassware, sample cell, and transfer lines were dried in a vacuum oven (65–85 °C) before use. Solution temperatures were measured with a Teflon-coated copper/constantan thermocouple inserted into the thermostatted sample compartment in close proximity to the sample cell. Substrates were added directly to the reservoir by microlitre syringe as aliquots of standard solutions.

Transient absorbance–time profiles were recorded by signal averaging of data obtained from 10–40 individual laser shots. Decay rate constants were calculated by nonlinear least-squares analysis of the transient absorbance–time profiles using the Prism 5.0 software package (GraphPad Software, Inc.) and the appropriate user-defined fitting equations, after importing the raw data from the Luzchem mLFP software. Rate and equilibrium constants were calculated by linear least-squares analysis of transient absorbance data that spanned as large a range in transient decay rate or initial signal intensity as possible. Errors are quoted in all cases as twice the standard error obtained from the least-squares analyses.

Steady-state photolysis experiments were carried out in quartz NMR tubes using a Rayonet® photochemical reactor (Southern New England Ultraviolet Co.) equipped with two RPP-2537 lamps and a merry-go-round apparatus, monitoring the solutions over selected time intervals by ^{1}H NMR spectroscopy. Cyclohexane-d_{12} solutions containing the desired combinations of germylene precursor and substrate and hexamethyldisilane (approximately 0.01 mol L^{-1}, internal integration standard) were prepared in 1 mL volumetric flasks. The solutions were then transferred to quartz NMR tubes, sealed with rubber septa, and then deoxygenated with a slow stream of dry argon for 5 min prior to irradiation over a total time period of 12–15 min. GC/MS analyses were carried out for each sample prior to and at the end of the photolysis period.

Theoretical calculations were carried out using the Gaussian09 suite of programs.[64]

Supplementary material

Supplementary material is available with the article through the journal Web site at http://nrcresearchpress.com/doi/suppl/10.1139/cjc-2014-0401.

Acknowledgements

We thank the Natural Sciences and Engineering Research Council of Canada for financial support, Teck Metals Ltd. for a generous donation of germanium tetrachloride, and Ian Duffy and Dr. Farahnaz Lollmahomed (McMaster University) for technical assistance.

References

(1) Yao, S.; Xiong, Y.; Brym, M.; Driess, D. *J. Am. Chem. Soc.* **2007**, *129*, 7268. doi:10.1021/ja072425s.
(2) Xiong, Y.; Yao, S.; Driess, M. *J. Am. Chem. Soc.* **2009**, *131*, 7562. doi:10.1021/ja9031049.
(3) Xiong, Y.; Yao, S.; Müller, R.; Kaupp, M.; Driess, M. *J. Am. Chem. Soc.* **2010**, *132*, 6912. doi:10.1021/ja1031024.
(4) Yao, S.; Xiong, Y.; Driess, M. *Chem. Eur. J.* **2010**, *16*, 1281. doi:10.1002/chem.200902467.
(5) Azhakar, R.; Pröpper, K.; Dittrich, B.; Roesky, H. W. *Organometallics* **2012**, *31*, 7586. doi:10.1021/om3008794.
(6) Filippou, A. C.; Baars, B.; Chernov, O.; Lebedev, Y. N.; Schnakenburg, G. *Angew. Chem. Int. Ed. Engl.* **2014**, *53*, 565. doi:10.1002/anie.201308433.
(7) Xiong, Y.; Yao, S.; Muller, R.; Kaupp, M.; Driess, M. *Nat. Chem.* **2010**, *2*, 577. doi:10.1038/nchem.666.
(8) Ghadwal, R. S.; Azhakar, R.; Roesky, H. W.; Pröpper, K.; Dittrich, B.; Klein, S.; Frenking, G. *J. Am. Chem. Soc.* **2011**, *133*, 17552. doi:10.1021/ja206702e.
(9) Tokitoh, N.; Matsumoto, T.; Okazaki, R. *Chem. Lett.* **1995**, *24*, 1087. doi:10.1246/cl.1995.1087.
(10) Li, L.; Fukawa, T.; Matsuo, T.; Hashizume, D.; Fueno, H.; Tanaka, K.; Tamao, K. *Nat. Chem.* **2012**, *4*, 361. doi:10.1038/nchem.1305.
(11) Belzner, J.; Ihmels, H.; Kneisel, B. O.; Herbst-Irmer, R. *Chem. Ber.* **1996**, *129*, 125. doi:10.1002/cber.19961290203.
(12) Tokitoh, N.; Matsumoto, T.; Manmaru, K.; Okazaki, R. *J. Am. Chem. Soc.* **1993**, *115*, 8855. doi:10.1021/ja00072a055.
(13) Suzuki, H.; Tokitoh, N.; Okazaki, R.; Nagase, S.; Goto, M. *J. Am. Chem. Soc.* **1998**, *120*, 11096. doi:10.1021/ja980783c.
(14) Iwamoto, T.; Sato, K.; Ishida, S.; Kabuto, C.; Kira, M. *J. Am. Chem. Soc.* **2006**, *128*, 16914. doi:10.1021/ja065774f.
(15) Tokitoh, N.; Okazaki, R.; Rappoport, Z. In *The Chemistry of Organic Germanium, Tin and Lead compounds, Vol. 2, Part 1*; Rappoport, Z., Ed.; John Wiley & Sons: New York, 2002; p. 843.
(16) Arrington, C. A.; West, R.; Michl, J. *J. Am. Chem. Soc.* **1983**, *105*, 6176. doi:10.1021/ja00357a048.
(17) Sandhu, V.; Strausz, O. P.; Bell, T. N. *Res. Chem. Intermed.* **1989**, *11*, 235. doi:10.1163/156856789X00357.
(18) Safarik, I.; Sandhu, V.; Lown, E. M.; Strausz, O. P.; Bell, T. N. *Res. Chem. Intermed.* **1990**, *14*, 105. doi:10.1163/156856790X00210.
(19) Becerra, R.; Frey, H. M.; Mason, B. P.; Walsh, R. *Chem. Phys. Lett.* **1991**, *185*, 415. doi:10.1016/0009-2614(91)80234-O.
(20) Goldberg, N.; Ogden, J. S.; Almond, M. J.; Walsh, R.; Cannady, J. P.; Becerra, R.; Lee, J. A. *Phys. Chem. Chem. Phys.* **2003**, *5*, 5371. doi:10.1039/b309871k.
(21) Becerra, R.; Walsh, R. *Phys. Chem. Chem. Phys.* **2007**, *9*, 2817. doi:10.1039/b617844h.
(22) Becerra, R.; Cannady, J. P.; Walsh, R. *J. Phys. Chem. A* **2002**, *106*, 4922. doi:10.1021/jp020091h.
(23) Takeda, N.; Tokitoh, N.; Okazaki, R. *Chem. Lett.* **2000**, 244. doi:10.1246/cl.2000.244.
(24) Soysa, H. S. D.; Okinoshima, H.; Weber, W. P. *J. Organomet. Chem.* **1977**, *133*, C17. doi:10.1016/S0022-328X(00)92880-8.
(25) Alnaimi, I. S.; Weber, W. P. *J. Organomet. Chem.* **1983**, *241*, 171. doi:10.1016/S0022-328X(00)98504-8.
(26) Madesclaire, M. *Tetrahedron* **1988**, *44*, 6537. doi:10.1016/S0040-4020(01)90096-1.
(27) Tzeng, D.; Weber, W. P. *J. Am. Chem. Soc.* **1980**, *102*, 1451. doi:10.1021/ja00524a054.
(28) Barton, T. J. *Pure Appl. Chem.* **1980**, *52*, 615. doi:10.1351/pac198052030615.
(29) Goure, W. F.; Barton, T. J. *J. Organomet. Chem.* **1980**, *199*, 33. doi:10.1016/S0022-328X(00)84519-2.
(30) Ando, W.; Ikeno, M.; Hamada, Y. *J. Chem. Soc., Chem. Commun.* **1981**, 621. doi:10.1039/C39810000621.
(31) Kostina, S. S.; Leigh, W. J. *J. Am. Chem. Soc.* **2011**, *133*, 4377. doi:10.1021/ja107881p.
(32) Castel, A.; Riviere, P.; Satge, J.; Cazes, A. *C. R. Acad. Sci. Paris Ser. C* **1978**, *287*, 205.
(33) Barrau, J.; Bouchaut, M.; Castel, A.; Cazes, A.; Dousse, G.; Lavayssiere, H.; Riviere, P.; Satge, J. *Synth. React. Inorg. Met.-Org. Chem.* **1979**, *9*, 273. doi:10.1080/00945717908057463.
(34) Barrau, J.; Bouchaut, M.; Lavayssiere, H.; Dousse, G.; Satge, J. *Helv. Chim. Acta* **1979**, *62*, 152. doi:10.1002/hlca.19790620122.
(35) Barrau, J.; Bouchaut, M.; Lavayssiere, H.; Dousse, G.; Satge, J. *J. Organomet. Chem.* **1983**, *243*, 281. doi:10.1016/S0022-328X(00)98549-8.
(36) Barrau, J.; Rima, G.; Lavayssiere, H.; Dousse, G.; Satge, J. *J. Organomet. Chem.* **1983**, *246*, 227. doi:10.1016/S0022-328X(00)98729-1.

(37) Kobayashi, S.; Iwata, S.; Abe, M.; Yajima, K.; Kim, H. J.; Shoda, S. *Makromol. Chem. Macromol. Symp.* **1992**, *54–55*, 225. doi:10.1002/masy.19920540119.
(38) Baggott, J. E.; Blitz, M. A.; Frey, H. M.; Lightfoot, P. D.; Walsh, R. *Int. J. Chem. Kinet.* **1992**, *24*, 127. doi:10.1002/kin.550240202.
(39) Su, M. D. *J. Am. Chem. Soc.* **2002**, *124*, 12335. doi:10.1021/ja020515l.
(40) Su, M. D. *J. Phys. Chem. A* **2002**, *106*, 9563. doi:10.1021/jp021176l.
(41) Apeloig, Y.; Sklenak, S. *Can. J. Chem.* **2000**, *78*, 1496. doi:10.1139/v00-107.
(42) Becerra, R.; Cannady, J. P.; Goulder, O.; Walsh, R. *J. Phys. Chem. A* **2010**, *114*, 784. doi:10.1021/jp908289h.
(43) Gillette, G. R.; Noren, G. H.; West, R. *Organometallics* **1987**, *6*, 2617. doi:10.1021/om00155a033.
(44) Gillette, G. R.; Noren, G. H.; West, R. *Organometallics* **1989**, *8*, 487. doi:10.1021/om00104a033.
(45) Kostina, S. S.; Singh, T.; Leigh, W. J. *Organometallics* **2012**, *31*, 3755. doi:10.1021/om3002558.
(46) Leigh, W. J.; Lollmahomed, F.; Harrington, C. R. *Organometallics* **2006**, *25*, 2055. doi:10.1021/om0600083.
(47) Lollmahomed, F.; Leigh, W. J. *Organometallics* **2009**, *28*, 3239. doi:10.1021/om9000814.
(48) Leigh, W. J.; Harrington, C. R.; Vargas-Baca, I. *J. Am. Chem. Soc.* **2004**, *126*, 16105. doi:10.1021/ja046308y.
(49) Leigh, W. J.; Harrington, C. R. *J. Am. Chem. Soc.* **2005**, *127*, 5084. doi:10.1021/ja043072p.
(50) Leigh, W. J.; Lollmahomed, F.; Harrington, C. R.; McDonald, J. M. *Organometallics* **2006**, *25*, 5424. doi:10.1021/om060595s.
(51) Huck, L. A.; Leigh, W. J. *Organometallics* **2007**, *26*, 1339. doi:10.1021/om0609362.
(52) Lee, C.; Yang, W.; Parr, R. G. *Phys. Rev. B* **1988**, *37*, 785. doi:10.1103/PhysRevB.37.785.
(53) Becke, A. D. *J. Chem. Phys.* **1993**, *98*, 5648. doi:10.1063/1.464913.
(54) Riviere, P.; Satge, J.; Castel, A. *C. R. Acad. Sci. Paris* **1975**, *281*, 835.
(55) Kira, M.; Ishida, S.; Iwamoto, T. *Chem. Record* **2004**, *4*, 243. doi:10.1002/tcr.20019.
(56) Tokitoh, N.; Ando, W. In *Reactive Intermediate Chemistry*; Moss, R. A., Platz, M. S., Jones, M., Jr., Eds.; John Wiley & Sons: New York, 2004; p. 651.
(57) Ando, W.; Itoh, H.; Tsumuraya, T. *Organometallics* **1989**, *8*, 2759. doi:10.1021/om00114a004.
(58) Schoeller, W. W.; Schneider, R. *Chem. Ber.* **1997**, *130*, 1013. doi:10.1002/cber.19971300731.
(59) Sakai, S. *Int. J. Quantum Chem.* **1998**, *70*, 291. doi:10.1002/(SICI)1097-461X(1998)70:2<291::AID-QUA5>3.0.CO;2-P.
(60) Heaven, M. W.; Metha, G. F.; Buntine, M. A. *J. Phys. Chem. A* **2001**, *105*, 1185. doi:10.1021/jp002873l.
(61) Lan, C.-Y.; Su, M.-D. *J. Phys. Chem. A* **2007**, *111*, 6232. doi:10.1021/jp072400f.
(62) Nag, M.; Gaspar, P. P. *Organometallics* **2009**, *28*, 5612. doi:10.1021/om900369e.
(63) Herzog, U.; Rheinwald, G. *J. Organomet. Chem.* **2001**, *627*, 23. doi:10.1016/S0022-328X(01)00707-0.
(64) Frisch, M. J.; Trucks, G. W.; Schlegel, H. B.; Scuseria, G. E.; Robb, M. A.; Cheeseman, J. R.; Scalmani, G.; Barone, V.; Mennucci, B.; Petersson, G. A.; Nakatsuji, H.; Caricato, M.; Li, X.; Hratchian, H. P.; Izmaylov, A. F.; Bloino, J.; Zheng, G.; Sonnenberg, J. L.; Hada, M.; Ehara, M.; Toyota, K.; Fukuda, R.; Hasegawa, J.; Ishida, M.; Nakajima, T.; Honda, Y.; Kitao, O.; Nakai, H.; Vreven, T.; Montgomery, J. A., Jr.; Peralta, J. E.; Ogliaro, F.; Bearpark, M.; Heyd, J. J.; Brothers, E.; Kudin, K. N.; Staroverov, V. N.; Kobayashi, R.; Normand, J.; Raghavachari, K.; Rendell, A.; Burant, J. C.; Iyengar, S. S.; Tomasi, J.; Cossi, M.; Rega, N.; Millam, N. J.; Klene, M.; Knox, J. E.; Cross, J. B.; Bakken, V.; Adamo, C.; Jaramillo, J.; Gomperts, R.; Stratmann, R. E.; Yazyev, O.; Austin, A. J.; Cammi, R.; Pomelli, C.; Ochterski, J. W.; Martin, R. L.; Morokuma, K.; Zakrzewski, V. G.; Voth, G. A.; Salvador, P.; Dannenberg, J. J.; Dapprich, S.; Daniels, A. D.; Farkas, Ö.; Foresman, J. B.; Ortiz, J. V.; Cioslowski, J.; Fox, D. J.; *Gaussian09*; Gaussian, Inc.: Wallingford, CT, 2009.